J Mol Model (2009) 15:829–836
DOI 10.1007/s00894-008-0437-2

ORIGINAL PAPER

A computational approach to studying monomer selectivity towards the template in an imprinted polymer

Siavash Riahi · Farrin Edris-Tabrizi · Mehran Javanbakht · Mohammad Reza Ganjali · Parviz Norouzi

Received: 8 August 2008 / Accepted: 22 November 2008 / Published online: 9 January 2009

Abstract A computational approach was proposed to study monomer–template interactions in a molecularly imprinted polymer (MIP) in order to gain insight at the molecular level into imprinting polymer selectivity, regarding complex formation between template and monomer at the pre-polymerisation step. This is the most important step in MIP preparation. In the present work, chlorphenamine (CPA), diphenhydramine (DHA) and methacrylic acid (MAA), were chosen as the template, non-template, and monomer, respectively. The attained complexes were optimised, and changes in the interaction energies, atomic charges, IR spectroscopy results, dipole moment, and polarisability were studied. The effects of solvent on template–monomer interactions were also investigated. According to a survey of the literature, this is the first work in which dipole moment and polarisability were used to predict the types of interactions existing in pre-polymerisation complexes. In addition, the density functional tight-binding (DFTB) method, an approximate version of the density functional theory (DFT) method that was extended to cover the London dispersion energy, was used to calculate the interaction energy.

S. Riahi (✉)
Institute of Petroleum Engineering,
Faculty of Engineering, University of Tehran,
P. O. Box 11365-4563, Tehran, Iran
e-mail: riahisv@khayam.ut.ac.ir

S. Riahi · M. R. Ganjali · P. Norouzi
Center of Excellence in Electrochemistry,
Faculty of Chemistry, University of Tehran,
P. O. Box 14155-6455, Tehran, Iran

F. Edris-Tabrizi · M. Javanbakht
Department of Chemistry, Amirkabir University of Technology,
Tehran, Iran

Keywords Chlorphenamine · Computational chemistry · Density functional theory · Molecularly imprinted polymer · Monomer-template interactions

Introduction

Molecularly imprinted polymer (MIP) is a kind of tailor-made material that has high affinity and selectivity for its template because of recognition sites formed in the polymer in the presence of the template. These sites remain after template removal, and remain able to rebind the template again. Combining the advantages of high selectivity, ease of preparation and economical synthesis, MIPs have recently attracted extensive attention [1].

MIPs have a great variety of applications, including chromatographic separations [2], molecularly imprinted solid phase extraction (MISPE) [3], sensors [4], drug delivery [5], membranes [6], and enantioseparation [7]. In addition, they are widely applied in biosensors in place of natural receptors and enzymes due to their superior stability and low cost [8–10].

MIP preparation is a simple procedure, but finding the best monomer, presenting the highest interaction with the template in order to achieve high selectivity and rebinding capacity is of great importance. Computational studies are useful methods with which to choose the most suitable monomers for imprinting polymers [11].

Dong et al. [12] chose the proper monomer to create the imprinted polymer of theophylline with the aid of computational methods. To evaluate the interactions between the template molecule and the monomer quantitatively, they measured the binding energy. Dineiro et al. [13] employed density functional theory (DFT) calculations to select the optimum functional monomer and porogenic solvent to

construct a recognition element for the dopamine metabolite homovanillic acid. In the studies conducted by Chianella et al. [3], molecular modelling based on the LEAPFROG algorithm was used to identify the best candidates for the molecular imprinting of abacavir. For the examination of MIP properties at the molecular level, Liu et al. [14] utilised the MMFF94 force field to calculate the interaction energies, which could be easily scaled-up for screening molecular imprinted systems. Monti et al. [15] used combined molecular dynamics (MD), molecular mechanics (MM), docking and site mapping computational techniques to simulate the formation of the possible imprinted polymers in an acetonitrile solution for theophylline. Indeed, in general, computational methods play a complementary role in experimental science [16–19].

The formation of a complex between the template molecule and the functional monomers in the pre-polymerisation step is the most effective step in MIP preparation, facilitating the polymerisation step [11]. MIPs prepared after a pre-polymerisation step demonstrate a higher selectivity and affinity toward the template.

In this study, an attempt was made to simulate the complex formed between the template/monomer and the non-template/monomer. Chlorphenamine (CPA) was chosen as template, its structural analogue diphenhydramine (DHA) as non-template, and methacrylic acid (MAA) as monomer. CPA is a histamine H1 antagonist of the alkyl amine family and is commonly used for the treatment of rhinitis, allergy, common cold, asthma and hay fever. DHA often co-exists with CPA in cough- and cold-syrups. As shown in Fig. 1, the structures of the two molecules are very similar. Since it is important to determine CPA in syrups and human serum to calculate optimal doses, a simple and economic way to separate and determine these two components is required. The CPA-imprinted polymer was prepared previously [20–22]. The reported data can be used to check the new methodology for the CPA imprinted polymer design. Although Mahato reported that CPA and DHA can be separated by reversed-phase ion-pair HPLC, this method is highly labour-intensive [23].

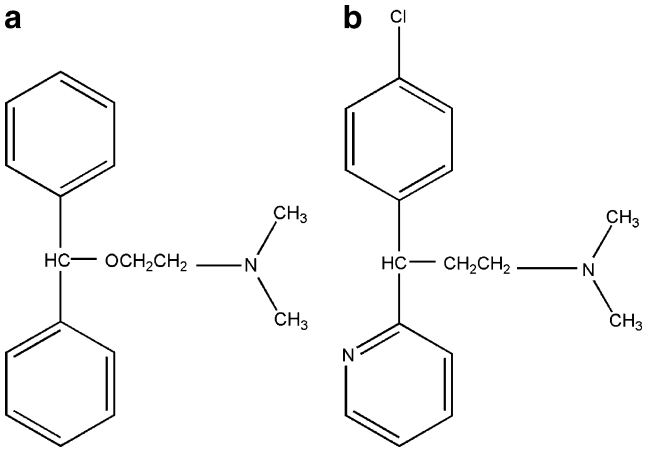

Fig. 1 Chemical structure of **a** diphenhydramine (DHA), and **b** chlorphenamine (CPA)

For the assessment of the template and monomer affinities, the binding energy (ΔE) of the template and the monomer can be used as a measure of their interaction [24–28]. As a new approach, additional parameters (e.g. changes in atomic charges, IR frequencies, dipole moment, and polarisability) were investigated. According to a survey of the literature, this is the first work in which the dipole moment and polarisability have been involved in predicting the interaction types that exist in pre-polymerization complexes. The estimation of MIP selective sites in such a way leads to the creation of a new method that identifies the interactions participating in imprinted sites.

Computational methods

Hardware and software

All computer simulations were undertaken at the Institute of Petroleum Engineering Supercomputer Center on a PC with an Intel Pentium 4, 3.20 GHz CPU, 4 GB memory, and 260 GB hard disk. The software used in this work consisted of HyperChem 5.1 [29], Gaussian 98 [30], and Gamess [31].

Geometry optimisation and energy calculation

In the first step, 3-D chemical structures of the monomer, template, and non-template were generated using HyperChem 5.1 software, which itself performed an initial optimisation using the AM1 method. The remaining calculations were then performed using Gaussian 98 software, which is an electronic structure package capable of predicting many properties, such as energies, structures, and vibrational frequencies, of atoms, molecules, and reactive systems. Full geometry optimisations and frequency calculations were performed and each species was found to be at minima by having no negative values in the frequency calculation.

The DFT calculation, which is commonly applied to MIP studies [11, 12, 32], has the advantages of high accuracy level of information, reliability, and reasonable computational costs in comparison with other computational methods (e.g. ab initio). Therefore, DFT was selected to set up the calculations. The geometry optimisations were performed at the B3LYP/6-311+(d,p) level—a type of DFT method that considers electronic correlation energy. This level usually provides better results for weak interaction systems compared with the Hartree-Fock method. Owing to the rather large size of CPA and DHA, the 6-311+(d,p)

basis set was quite satisfactory for this study. In addition, the density functional tight-binding (DFTB) theory was used in order to obtain more precise and reliable results. The DFTB methods are a group of precise quantum mechanical (QM) calculations for computational studies and include the empirical London dispersion energy term DFTB-D, which has been proved very suitable and accurate for calculations of interaction energy and H-bonding [33].

Results and discussion

Figure 2 shows a schematic representation of molecular imprinting steps including polymer synthesis and template removal. The cavity with functional groups complementary to template remains after template removal, thus the template can rebind the polymer again.

Complex formation

Traditionally, MIPs have been divided in two main categories—covalent and non-covalent—based on the types of interaction existing between the template and the monomer. However, the non-covalent approach is used more extensively. In non-covalent MIPs, there is no need for the synthetic step in monomer–template complex formation, and template removal is easier during the washing step [34].

In a non-covalent MIP, the interactions contributing to ΔE between the template and the monomers are ionic bonds, hydrogen bonds, van der Waals interactions, and dipole–dipole interactions. In order to investigate the selectivity of the monomers to the template, it was necessary to consider all the above-mentioned interactions.

As indicated in several previous studies, hydrogen bonding is the most important interaction in non-covalent imprinted polymers [11, 35]. Thus, in this study, complex level was determined by the number of hydrogen bonds formed between the functional monomer and the template, or non-template. CPA has three main functional groups, all of which are proton acceptors, while DHA has two functional groups. Consequently, these molecules can possibly participate in three and two hydrogen bonds, respectively. CPA-MAA (1:1), CPA-MAA (1:2), CPA-MAA (1:3), DHA-MAA (1:1), and DHA-MAA (1:2) complexes were optimised. The optimised structures of MAA, CPA, and DHA are shown in Fig. 3.

Prior to set (1:1) complex optimisation, a scan was done to determine the best interaction site between template and monomer.

Therefore, DFT calculations were performed at different angles between template and monomer. For each angle, the

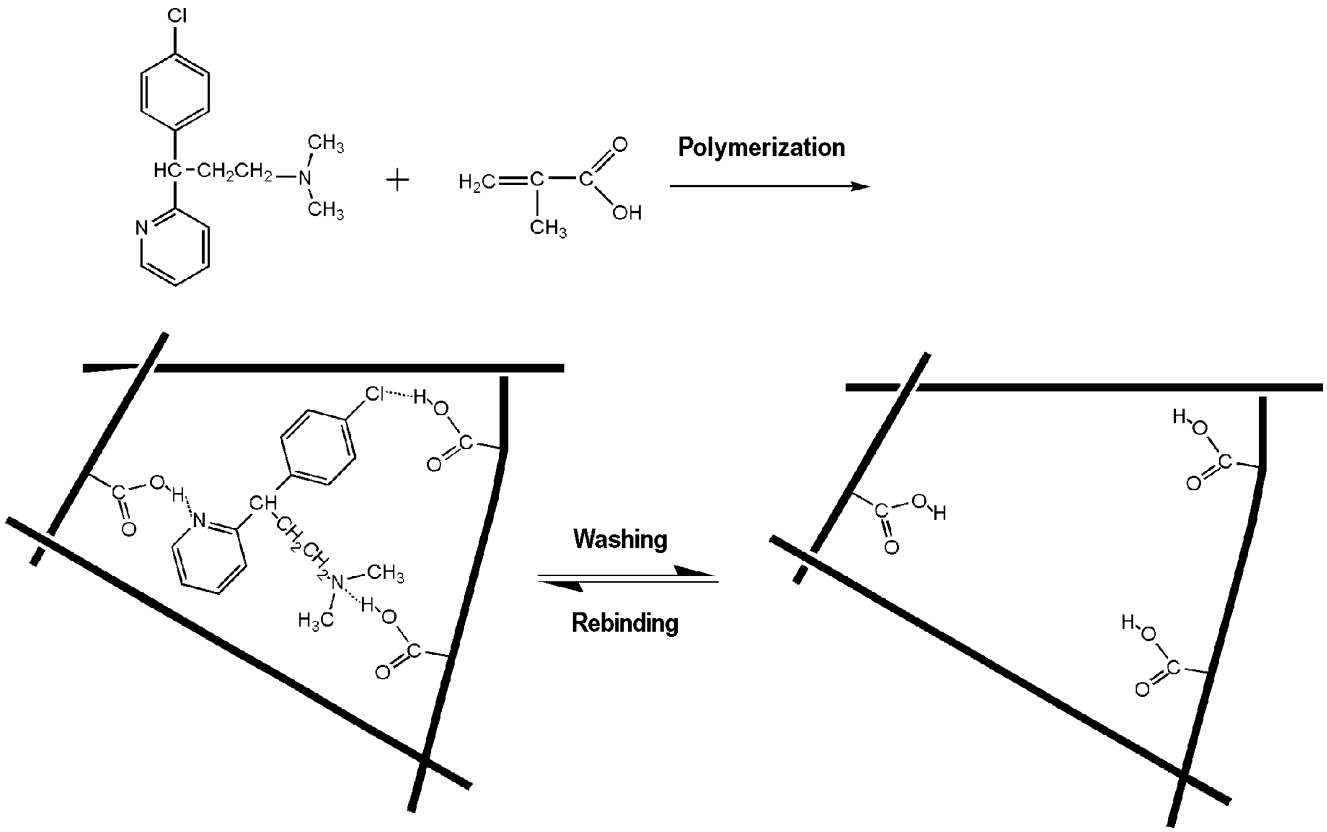

Fig. 2 Schematic representation of the imprinting polymer process

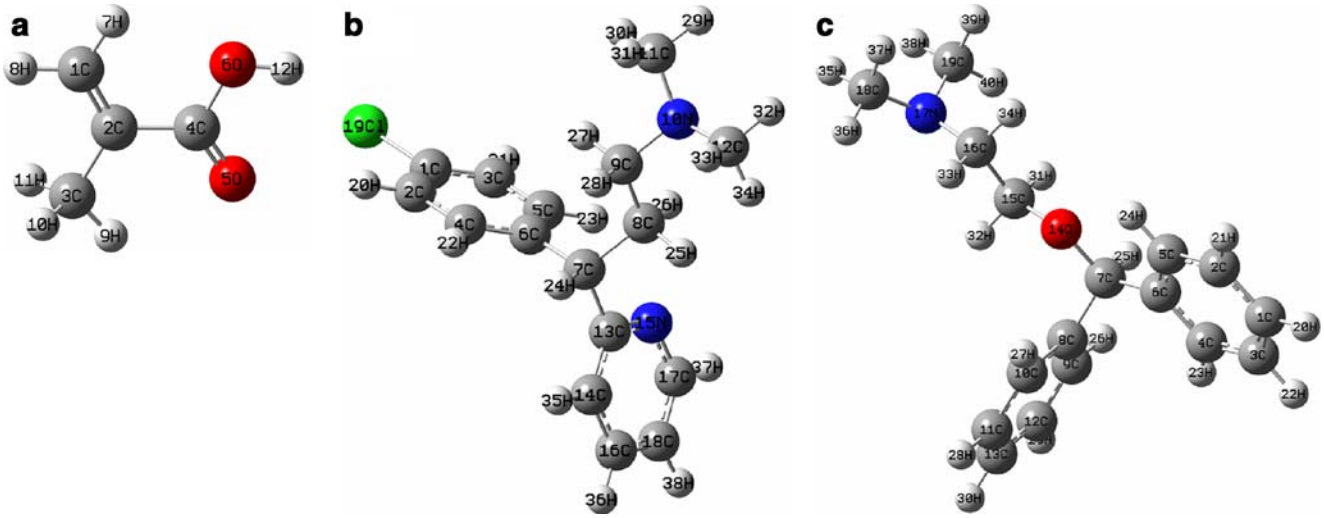

Fig. 3 Optimised structures of **a** methacrylic acid (MAA), **b** CPA, **c** DHA

corresponding energy was calculated and the optimised angle obtained. The interaction energies between the monomer(s) and the template or its analogue were calculated to quantitatively assess the interaction between the studied molecules.

ΔE calculations

Firstly, the geometry optimisation and the energy calculation were performed for the template, the non-template, and the monomer individually. The obtained structures were applied to the complexes formed between the template or its analogues and the monomers. The interaction energies of the template with the monomer(s) can be calculated from Eq. 1:

$$\Delta E = \left| \begin{matrix} E(complex) - E(template\,or\,non-template) \\ -\Sigma E(monomers) \end{matrix} \right| \quad (1)$$

The calculated values are listed in Table 1. According to earlier studies, complexes with higher ΔE provide MIPs with higher selectivity [1, 11–13]. From the results in Table 1, it can be concluded that the order of the molecular interactions is as follows: CPA-MAA (1:3) >CPA-MAA (1:2) > DHA-MAA (1:2) > CPA-MAA (1:1) > DHA-MAA (1:1). These results show that CPA-MAA (1:3) is the most stable complex, and that CPA interacts strongly with the three MAA molecules. The basis set superposition error (BSSE), which often substantially affects the calculated stabilisation energies, was corrected by means of the counterpoise method [36, 37]. The interaction energies changed a little after BSSE correction. For example, the values changed from 65.409 to 67.527 kcal mol^{-1} for CPA-MAA (1:3) and from 31.055 to 32.984 kcal mol^{-1} for DHA-MAA (1:2). The order of interaction energies remained the same.

Figure 4 depicts the optimised structures of CPA-MAA (1:3) and DHA-MAA (1:2). For clarity, Fig. 4 shows only those hydrogen atoms with large atomic charge alterations.

In the experimental study reported for CPA imprinted polymer, the selectivity of the imprinted polymer was evaluated by comparing the retention of CPA and its structural analogue diphenhydramine on an HPLC column packed with the CPA imprinted polymer [20]. The capacity factor of CPA on the imprinted polymer was 4.68, but for diphenhydramine it was only 0.405 [20]. The higher capacity factor for CPA shows the selectivity of MIP toward CPA; our computational results also show a higher interaction energy between CPA and MAA. Therefore, these experimental results confirm the reliability of our computational method.

Table 1 Binding energies between the template, the non-template and the monomer(s)

	Energy (Hartree/particle)	ΔE (interaction energy) in gas phase (kcal/mol)	ΔE (interaction energy) in solvent (kcal/mol)
MAA	306.284	–	
CPA	1,190.284	–	
DHA	789.839	–	
CPA-MAA	1,496.595	16.678	27.458
CPA-$(MAA)_2$	1,802.906	33.726	64.259
CPA-$(MAA)_3$	2,109.241	65.409 (69.254)[a]	97.321
DHA-MAA	1,096.149	16.177	24.957
DHA-$(MAA)_2$	1,402.458	31.055 (34.841)[a]	52.294

MAA Methacrylic acid, *CPA* chlorphenamine, *DHA* diphenhydramine
[a] Values in brackets represent interaction energies calculated by the density functional tight-binding (DFTB) method

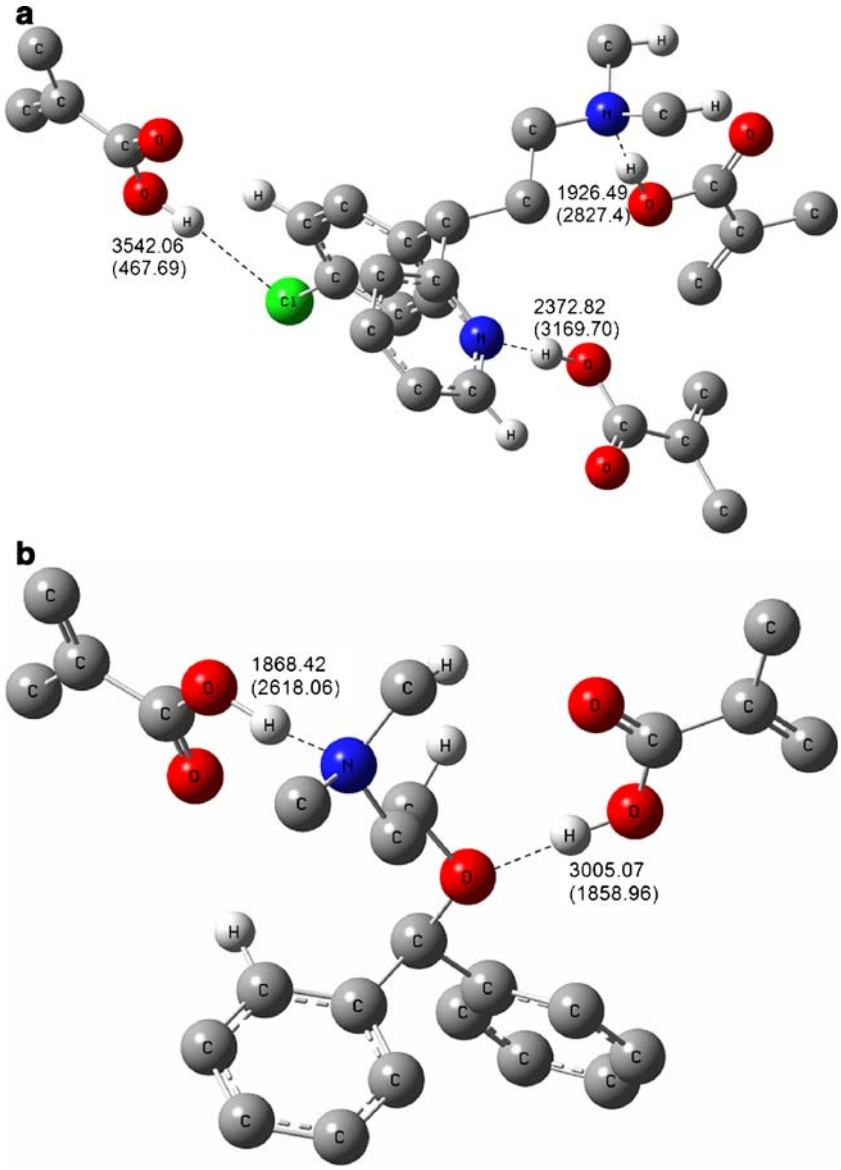

Fig. 4 **a** The (1:3) complex formed between CPA and MAA. **b** The (1:2) complex formed between DHA and MAA. The frequencies (cm^{-1}) and intensities (values in parenthesis) of O–H bond stretching after complex formation are indicated

Atomic charges

Table 2 summarises the atomic charges in CPA and DHA. It should be mentioned that, to avoid presenting a large amount of data, only those atoms exhibiting significant changes in their atomic charges after complex formation are shown in the table. The atomic charges of atoms participating in complex formation changed more significantly in comparison with those of other atoms (Fig. 4). From these changes, it was deduced that, in CPA and DHA, atoms participating in final complex formation were N_{10}, N_{15}, Cl_{19} H_{20}, H_{29}, H_{37} and N_{17}, O_{14}, H_{31}, and H_{32}, respectively. Furthermore, to select the most stable complex, the changes in atomic charges in the interaction sites were compared before and after complex formation. As the interactions between the monomer and the template become stronger, the changes in the atomic charges increase. It was obvious that the charge variation after complex formation was more significant in CPA-MAA (1:3) than in DHA-MAA (1:2).

IR vibration

The vibrational frequencies of MAA, CPA, and DHA before and after complex formation at the B3LYP/6 31G level of theory were calculated.

The O–H group on MAA is the most important functional group in hydrogen bonding. The single monomer is considered a peak, representing the O–H stretching bond located at 3,630.48 cm^{-1} and 41.428 intensity. Depending on the strength of hydrogen bonding formed between MAA and CPA or DHA, the peak intensity increases and shifts to lower frequencies. Figure 4a and b show the changes of O–

Table 2 Atomic charges in CPA and DHA before and after complex formation

			Atomic charge			
	No.	Atom	Individual	(1:1) complex	(1:2) complex	(1:3) complex
CPA	2	C	**−0.0991**	−0.0963	−0.0963	**−0.121**
	10	N	**−0.4419**	−0.4413	**−0.5855**	−0.5870
	13	C	**0.2099**	**0.3186**	0.3149	0.315
	15	N	**−0.4182**	**−0.6099**	−0.6063	−0.6081
	17	C	**0.0096**	**0.0697**	0.0700	0.0700
	19	Cl	**0.0516**	0.0581	0.0631	**0.0342**
	20	H	**0.1543**	0.1562	0.1575	**0.2144**
	29	H	**0.1402**	0.1416	**0.1990**	0.1994
	32	H	**0.1420**	0.1437	**0.1991**	0.1989
	37	H	**0.1456**	**0.2181**	0.2185	0.2184
DHA	7	C	**−0.0261**	−0.0303	**−0.0564**	-
	14	O	**−0.5436**	−0.5468	**−0.5895**	-
	15	C	**0.0146**	−0.0044	**−0.0696**	-
	17	N	**−0.4501**	**−0.5840**	−0.5944	-
	31	H	**0.1203**	0.1478	**0.1780**	-
	32	H	**0.1505**	0.1651	**0.2053**	-
	40	H	**0.1423**	**0.2048**	0.2055	-

H stretching bond values after complex formation. The values before brackets represent the frequencies (cm^{-1}) and the values inside brackets represent the intensities. It is obvious that O–H stretching frequency moved to lower frequencies after complex formation, and this is more marked in CPA-MAA (1:3) than in DHA-MAA (1:2).

Dipole moment and polarisability

Dipole moment and polarisability values were another proof of the functional monomer tendency toward the CPA molecule. Polarisability is the relative tendency of a charge distribution, like the electron cloud of an atom or molecule, to be distorted from its normal shape by an external electric field. Dipole moment refers to the quality of a system to behave like a dipole. Dipole moment is the measured polarity of a polar covalent bond and is defined as the product magnitude of charge on the atoms and the distance between the two bonded atoms. The initial step in formation of a complex is the similarity of some physical properties in the species, which is necessary for specific and tight binding. The 3D electrostatic field surrounding each molecule plays a crucial role in this step. When molecules approach each other, the initial contact arises from long-range electrostatic forces, which can be separated into three interactions: electrostatic, inductive, and dispersive. The first type of interaction is more effective than the others and appears between polar molecules that carry charge or possess a permanent dipole moment.

Table 3 shows the dipole moment and polarisability of the monomer, the template, and the non-template. All three molecules are polar. The presence of a heterogeneous atom at the end of the structure (like the Cl atom in CPA) pulls the electrostatic field surrounding the molecule and increases the dipole moment. Therefore, the dipole moment of CPA is greater than that of DHA, which means that CPA creates a stronger dipole–dipole interaction with polar compounds than DHA.

In line with the polarisability and the dipole moment, the type of interaction in CPA is dipole–dipole, whereas in DHA dispersion interaction took place. Since the dipole–dipole interaction is stronger than that of dispersion, the monomers selectivity to the CPA template is greater in comparison to that towards the DHA template.

Computer simulation in solvent

Solvents with various dielectric constants and hydrogen bonding capacities influence the template/monomer interaction differently. Thus, in this study we set up a single point calculation in order to investigate the solvent (chloroform) effect on template/monomer non-covalent interactions. We chose chloroform because it was used as a solvent in former experimental work [20]. The conformations obtained in gas phase were used to calculate the interaction energies in chloroform from Eq. 1, and the

Table 3 Dipole moment and polarisability of the monomer, the template and the non-template

	Dipole moment (Debye)	Polarisability
MAA	1.777	57.299
CPA	4.398	169.091
DHA	1.138	204.633

obtained ΔE values reported in Table 1 confirm that chloroform increased monomer/template interactions in comparison to those of the gas phase. Since chloroform is an aprotic solvent with low dielectric constant, it is likely to lead to large interaction energy between the template and the functional monomer [32].

Conclusions

This work presents a computational model for the study of MIP selectivity. Chlorphenamine was chosen as a template to examine the validity of this approach. The interaction energies, dipole moment, polarisability, and IR spectroscopy results obtained from the computational optimisation indicated that CPA was more strongly bonded to the monomer in comparison with its analogue DHA, and each template molecule interacted with three functional monomers. Moreover, atomic charge alterations before and after complex formation provided details about the atoms taking part in hydrogen bonding.

In the field of molecular imprinting, the number of articles based on computational predictions is limited in comparison with articles describing experimental studies. We believe that rational computational MIP design in its various steps is safe, economical, consumes no reagents, and can be used instead of the trial and error method. In order to find the best monomer for a particular template, it is easy and economical to calculate the interaction energies between the template and different monomers in solution before MIP synthesis.

Acknowledgement We gratefully acknowledge the generous allocation of computing time from the Institute of Petroleum Engineering, University of Tehran for Advanced Computing and Supercomputing Facilities.

References

1. Wu L, Li Y (2004) Study on the recognition of templates and their analogues on molecularly imprinted polymer using computational and conformational analysis approaches. J Mol Recognit 17: 567–574
2. Haginaka J, Sanbe H (2001) Uniformly sized molecularly imprinted polymer for (S)-naproxen—retention and molecular recognition properties in aqueous mobile phase. J Chromatogr A 913:141–146
3. Chianella I, Karim K, Piletska EV et al (2006) Computational design and synthesis of molecularly imprinted polymers with high binding capacity for pharmaceutical applications-model case: adsorbent for abacavir. Anal Chim Acta 559:73–78
4. Haupt K, Mosbach K (2000) Molecularly imprinted polymers and their use in biomimetic sensors. Chem Rev 100:2495–2504
5. Ciardelli G, Cioni B, Cristallini C et al (2004) Acrylic polymeric nanospheres for the release and recognition of molecules of clinical interest. Biosens Bioelectron 20:1083–1090
6. Donato L, Figoli A, Drioli E (2005) Novel composite poly (4-vinylpyridine)/polypropylene membranes with recognition properties for (S)-naproxen. J Pharm Biomed Anal 37:1003–1008
7. Sambe H, Hoshina K, Moaddel R et al (2006) Uniformly-sized, molecularly imprinted polymers for nicotine by precipitation polymerization. J Chromatogr A 1134:88–94
8. Ozcan L, Sahin Y (2007) Determination of paracetamol based on electropolymerized-molecularly imprinted polypyrrole modified pencil graphite electrode. Sens Actuators B 127:362–369
9. Gomez-Caballero A, Unceta M, Goicolea MA et al (2007) Evaluation of the selective detection of 4,6-dinitro-*o*-cresol by a molecularly imprinted polymer based microsensor electrosynthesized in a semi-organic media. Sens Actuators, B. 130:713–722
10. Holthoff EL, Bright FV (2007) Molecularly templated materials in chemical sensing. Anal Chim Acta 594:147–161
11. Piletsky SA, Karim K, Piletska EV et al (2001) Recognition of ephedrine enantiomers by molecularly imprinted polymers designed using a computational approach. Analyst 126:1826–1830
12. Dong W, Yan M, Zhang M et al (2005) A computational and experimental investigation of the interaction between the template molecule and the functional monomer used in the molecularly imprinted polymer. Anal Chim Acta 542:186–192
13. Dineiro Y, Menendez MI, Blanco-Lopez MC et al (2006) Computational predictions and experimental affinity distributions for a homovanillic acid molecularly imprinted polymer. Biosens Bioelectron 22:364–371
14. Liu Y, Wang F, Tan TW et al (2007) Study of the properties of molecularly imprinted polymers by computational and conformational analysis. Anal Chim Acta 581:137–146
15. Monti S, Cappelli C, Bronco S et al (2006) Towards the design of highly selective recognition sites into molecular imprinting polymers: a computational approach. Biosens Bioelectron 22:153–163
16. Riahi S, Ganjali MR, Norouzi P et al (2008) Application of GA-MLR, GA-PLS and the DFT quantum Mechanical (QM) calculations for the prediction of the selectivity coefficients of a histamine-selective electrode. Sens Actuators B 132:13–19
17. Riahi S, Norouzi P, Bayandori-Moghaddam A et al (2007) Theoretical and experimental report on the determination of electrode potentials of dihydroxyanthracene and thioxanthens derivatives. Chem Phys 337:33–38
18. Riahi S, Ganjali MR, Bayandori-Moghaddamb A et al (2008) Structural study of 2-(1-oxo-1 H-inden-3-yl)-2H-indene-1,3-dione by ab initio and DFT calculations, NMR and IR spectroscopy. Spectrochim Acta, Part A 70:94–98
19. Riahi S, Ganjali MR, Bayandori-Moghaddam A et al (2006) Determination of the electrode potentials for substituted 1,2-dihydroxybenzenes in aqueous solution: theory and experiment. J Mol Struct (THEOCHEM) 774:107–111
20. Chen W, Liu F, Zhang X et al (2001) The specificity of a chlorphenamine-imprinted polymer and its application. Talanta 55:29–34
21. Haginaka J, Kawaga C (2002) Uniformly sized molecularly imprinted polymer for d-chlorpheniramine - Evaluation of retention and molecular recognition properties in an aqueous mobile phase. J Chromatogr A 948:77–84
22. Haginaka J, Kawaga C (2004) Retentivity and enantioselectivity of uniformly sized molecularly imprinted polymers for d-chlorpheniramine and -brompheniramine in hydro-organic mobile phases. J Chromatogr B 804:19–24
23. Mahato SB, Sahu NP, Maitra SK (1986) Simultaneous determination of chlorpheniramine and diphenhydramine in cough syrups by reversed-phase ion-pair high-performance liquid chromatography. J Chromatogr 351:580–584
24. Riahi S, Ganjali MR, Moghaddam AB (2008) Experimental and quantum chemical study on the IR, UV and electrode potential of 6-(2,3-dihydro-1,3-dioxo-2-phenyl-1*H*-inden-2-yl)-2,3-dihydroxybenzaldehyde. Spectrochim Acta, Part A 71:1390–1396

25. Ganjali MR, Norouzi P, Faridbod F et al (2007) Determination of Vanadyl ions by a New PVC Membrane Sensor Based on N, N'-bis-(salicylidene)-2,2-dimethylpropane-1,3-diamine. IEEE Sens J 7:544–550
26. Ganjali MR, Norouzi P, Mirnaghi FS (2007) Lanthanide recognition: monitoring of praseodymium(III) by a novel praseodymium (III) microsensor based on N-(pyridine-2-ylmethylene) benzohydrazide. IEEE Sens J 7:1138–1144
27. Faridbod F, Ganjali MR, Larijani B (2007) Lanthanide recognition: an asymetric erbium microsensor based on a hydrazone derivative. Sensors 7:3119–3135
28. Faridbod F, Ganjali MR, Dinarvand R (2008) Schiff's bases and crown ethers as supramolecular sensing materials in construction of the potentiometric membrane sensors. Sensors 8:1645–1703
29. HyperChem™ (1997) Molecular Modeling System, Release 5.1 Pro for Windows, Hypercube Inc, Gainesville, FL
30. Frisch MJ, Trucks GW, Schlegel HB et al (1998) Gaussian Inc, Pittsburgh, PA
31. Schimdt MW et al (1993) J Comput Chem 14:1347–1355
32. Wu L, Zhu K, Zhao M et al (2005) Theoretical and experimental study of nicotinamide molecularly imprinted polymers with different porogens. Anal Chim Acta 549:39–44
33. Elstner M, Hozba P, Frauenheim T et al (2001) Hydrogen bonding and stacking interactions of nucleic acid base pairs: a density-functional-theory based treatment. J Chem Phys 114:5149–5155
34. Spivak A (2005) Adv Drug Deliver Rev 57:1779
35. Karim K, Breton F, Rouillon R et al (2005) Adv Drug Deliver Rev 57:1795
36. Schwenke DW, Truhlar DG (1985) J Chem Phys 82:2418–2423
37. Frisch MJ, Del Bene JE, Binkley JS et al (1986) Extensive theoretical studies of the hydrogen-bonded complexes $(H_2O)_2$, $(H_2O)_2H^+$, $(HF)_2$, $(HF)_2H^+$, F_2H^-, and $(NH_3)_2$. J Chem Phys 84:2279–2289